Analysis of Structural and Antibacterial activity on Mg doped Hydroxyapatite

S.Saranya, B.Rajalakshmi, S.Meenakshi M.Prema Rani *

**Research Centre PG Department of Physics,* The *Madura College, Madurai-11, Tamilnadu, India.*
e-mail:saranyaashok122012@gmail.com

Abstract

Mg substituted HAp samples with variable amounts of Mg were synthesized by sol–gel method. The samples were sintered in the furnace at 600º C for 2 hrs. The samples were characterized by Fourier Transform Infrared Spectroscopy for functional group analysis, X-Ray Diffraction for crystallinity and phase purity analysis. The FTIR shows the influence of Mg and XRD results confirmed presence of Mg in the lattice structure of HAp. The crystal size is found to be in the range of 19nm-21nm. The EDX results confirmed the elemental composition of the doped and undoped samples. Antibacterial activity taken against the bacteria Shigella flexneri shows that activity increases with the addition metal dopant Mg.

Keywords: Hydroxyapatite, FTIR, Magnesium, Sol gel, XRD, Antimicrobial activity

1. Introduction:

Bone tissue has a regenerative capacity for self repair on damage. This self repairing process often fails when the bone defects are too large or the natural healing capacity is insufficient [1-4]. The recent strategies for reconstructing these large bone defects use bone grafting materials such as autografts and xenografts. The limitations in those approaches viz., the limited availability and poor biocompatibility have all increased the necessity of artificial synthetic bone implants incorporating ceramics like calcium phosphate materials on its surface . The biomineral phase, which is one or more type of calcium phosphates, comprises 65-70% of bone, water accounts for 5-8% and the organic phase, like collagen, accounts for the remainder [5-9]. Thus it is commonly used as filler for amputated bone or coating to promote bone in growth over the prosthetic implants [10].Important techniques being used are solid state reaction, co-precipitation, emulsion, etc., and produce HAp in different forms. Magnesium (Mg) is known to be an important trace element, particularly during in osteogenesis where it stimulates osteoblast

proliferation and its depletion causes bone fragility and bone loss [11]. Furthermore, relationship has been suggested between the Mg content in enamel and the development of dental caries.The primary objective of this study is the incorporation of Mg ion in HAp by sol-gel method to explore the impact of the Mg concentration on HAP crystal structure. The biological apatite differs from pure HA in terms of stoichiometry, solubility, crystallinity, composition and other biological and mechanical properties. The most interesting research objective is developing new biomaterials that better the bone mineral features [12]. Magnesium (Mg) is quantitatively the most important bivalent element associated with biological apatite and cells [13]. Magnesium ions help in bone mineralization through osteoblast activity [14]. Mg addition has an inhibitory effect on HAP nucleation and growth [15]. It has significant contribution in preventing possible risk factors of osteoporosis in humans [16, 17–19]. The use of metal ions as dopants can determine an augmentation of HAp interactions in cells, and increases the mechanical properties of HAP [20, 21]. The Mg-doped HAp has importance in the development of artificial bone substitutes. This is owned to the fact that Mg^{2+} combined with calcium phosphates exhibits important role during the spontaneous formation in vivo bone bonding and closely associated with the mineralization of calcified tissues [22, 23, 24]. This study says Mg is a key factor in the qualitative development of the bone matrix. [25, 26].

2. Experimental Procedure

Calcium nitrate tetra hydrate ($Ca(NO_3)_2.4H_2O$) was mixed with ethanol and phosphorous pentaoxide P_2O_5 and the solution was stirred in a magnetic stirrer for about 40 mins. After the formation of gel the sample was dried at 120ºC for 2 hours. A gelation was formed which was dried out by further heating. The dried samples were ground using mortar and pestle. The sample was sintered in the furnace at 600º C for 2 hrs. The final product formed was obtained as fine white powder.

To Obtain Mg doped HAp

Mg-doped hydroxyapatite with different concentration [where x= 0.05%, 0.10%] of 0.1M was synthesized by sol-gel method. The preparation of pure HAp was done by dissolving stoichiometric amount of calcium nitrate tetrahydrate and Phosphorus pentaoxide in 50ml of ethanol in a separate beaker. Both the mixture was stirred for 40 minutes. Magnesium doped hydroxyapatite was prepared by dissolving stoichiometric amount of calcium nitrate tetrahydrate,

Magnesium nitrate hexahydrate (Mg $(NO3)_2$.6H2O) and phosphorus pentaoxide in ethanol .The mixture of sol was stirred vigorously on a magnetic stirrer for 40 minutes for uniform mixing. The resultant gel of both doped and undoped HAp was kept in water bath for 2hrs to obtain precipitate. The gel was heated at 120°C to obtain dry powder. The obtained powder was then annealed at 600°C for 2hrs. Finally a white powder was obtained.

3. Results and discussion

3.1 X-ray diffraction (XRD)

The structural characterization has been done by XRD. X- ray powder diffraction measurements was performed at SAIF (Sophisticated Analytical Instrument Facility), Cochin using $CuK\alpha_1$ with 2θ range from 10^0 to 120^0 and 0.02^0 step sizes. The comparative XRD profiles are given in figure 1. The intensity of the Mg doped samples decrease with concentration. This may be due to the lower atomic number of Mg (12) compared to that of Calcium (20). The XRD profiles were compared with JCPDS data from JCPDS [pdf No. #460905] which confirmed the hexagonal structure of the crystals. The lattice parameters from software unit cell have been tabulated in table 2. The crystallite size was calculated from full-width-at-half-maximum (FWHM) for the diffraction peaks. The crystallite size calculated for the samples is shown in table1. The crystallite size of the doped samples decrease with respect to pure HAp which may be due to the larger atomic radius of Mg (145 pm) when compared with Calcium (194 pm).

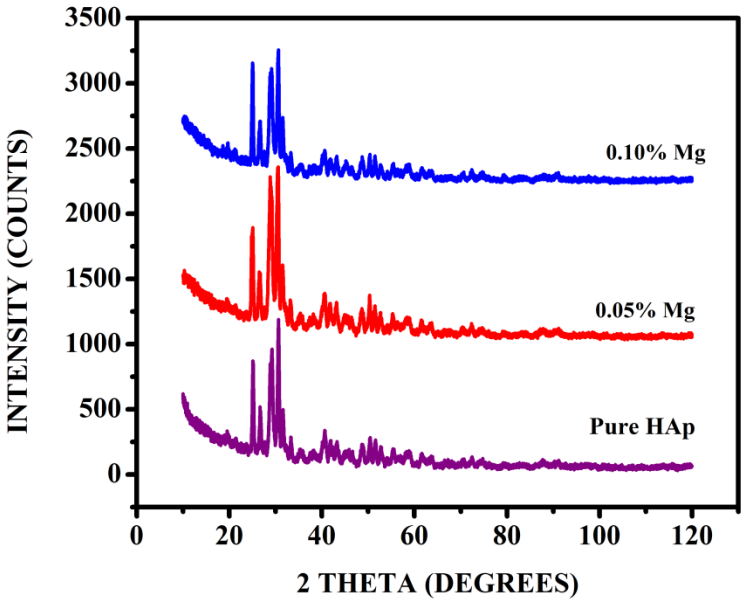

Fig1 XRD profile of $Ca_{10-x}Mg_x(PO_4)_6(OH)_2$ [x=0,0.05,0.10,] nanostructures.

Table 1 Crystallite size of $Ca_{10-x}Mg_x(PO_4)_6(OH)_2$ [x=0,0.05,0.10] nanostructures.

S.No.	$Ca_{10-x}Mg_x(PO_4)_6(OH)_2$	Crystallite size (nm)
1	X=0	21.22
2	X=0.05	20.11
3	X=0.10	19.83

Table 2 DETERMINATION OF LATTICE PARAMETERS FROM UNIT CELL

Sample	Lattice parameters (Å)		Volume $(Å)^3$
X=0	9.4407 (0.0001)	6.8811 (0.0001)	531.1199 (0.0092)
X=0.05	9.4406 (0.0000)	6.8810 (0.0002)	531.1148 (0.0118)
X=0.10	9.4407 (0.0000)	6.8809 (0.0000)	531.1123 (0.0042)

3.2 FOURIER TRANSFORM INFRARED SPECTROSCOPY

FTIR data was collected from Kalasalingam University, Research centre Department of physics, Krishnanakoil Tamil Nadu. The presence of functional groups was confirmed using Fourier transform infrared spectroscopy. The spectrum was recorded in the

range of 400–4000 cm^{-1} using KBr pellet technique. The resolution of spectrometer was $4cm^{-1}$. The representative FTIR spectrum shows all characteristic absorption peaks of HAp. The Comparative FTIR Profile is shown in figure 2. Functional Group Analysis of doped samples are shown in table 3.The characteristic bands of phosphate and hydroxyl groups, as well as carbonate groups, were detected from the FTIR spectra of the samples. The absorption band around $1643cm^{-1}$ is attributed to the presence of CO_3^{2-} in all the samples. The intense broad peak between 942 cm^{-1} and1029 cm^{-1} is assigned to PO_4^{3-} in samples The peak observed around 3462 cm^{-1} is the characteristic peak corresponding to stoichiometric HAp. The Mg doped HAp shows decreased intensity of OH vibration modes at those bands with respect to HAp samples. It can be explained by the increased lattice due to HPO_4^{2-}substitution.

Table 3 Transmittance data of $Ca_{10-x}Mg_x(PO_4)_6(OH)_2$ [x=0,0.05,0.10] nanostructures.

Chemical group	X= 0	X= 0.05	X= 0.10	**Remarks**
OH^-	3570.2	3570.24	3570.24	Presence of HAp
OH^-	3423.6	3417.86	3514.93	Decreases with incresae in dopant concentration
HPO_4^{2-}	601.79	603.72	603.72	Increases due to doping of Ce

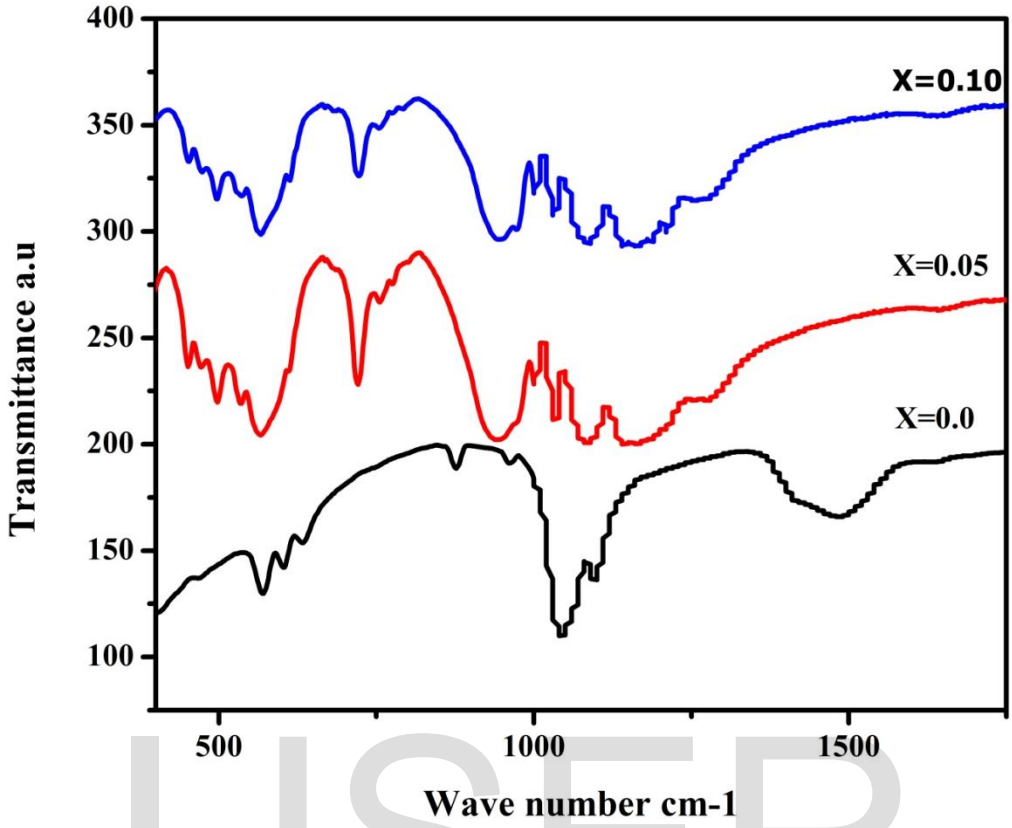

Fig 2 FTIR graph of $Ca_{10-x}Mg_x(PO_4)_6(OH)_2$ [x=0.0,0.05,0.10] nanostructures.

3.3 EMISSION DISPERSIVE SPECTROSCOPY

From EDS spectra verify the elemental compositions, were verified and no impurity is observed for all the samples. Most importantly, the Mg doping process causes the Ca-deficiency. At higher amounts of the Mg dopants, the Ca deficiency increases significantly. In other words, it may be due to the ionic substitution, which may be occurred due to crystal defect, between Mg and Ca. The EDS figures of HAp and Mg doped HAp are shown in the figures 3a-3c. The elements present in the samples are tabulated in the table 4. This table shows that Mg has been doped well in the crystal lattice.

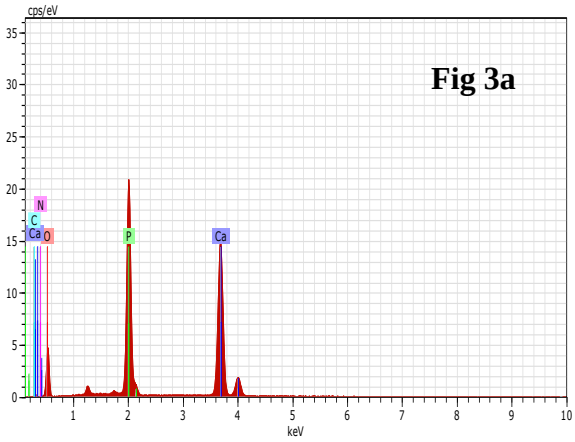

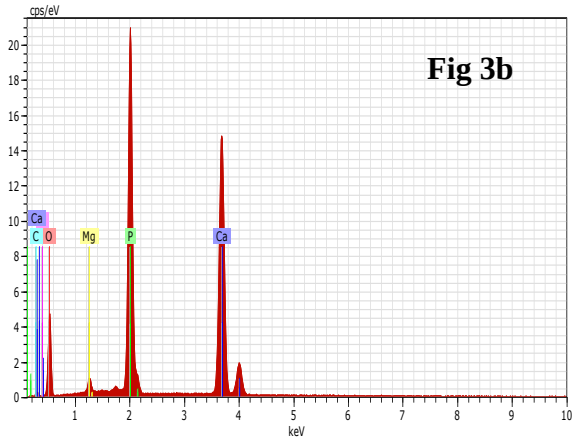

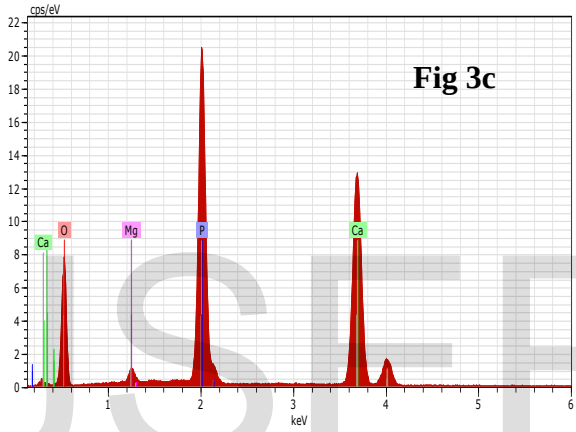

Figures 3a-3c. EDS images of $Ca_{10-x}Mg_x(PO_4)_6(OH)_2$ [x=0.0, 0.05, 0.10] nanostructures respectively.

Table 4 EDS Analysis for HAp and Mg doped HAp

Samples	Ca	P	O	Mg
X= 0.0	26.51	21.54	56.98	-
X= 0.05	25.38	20.73	57.29	1.09
X= 0.10	22.87	23.86	63.89	1.74

3.4 TRANSVERSE ELECTRON MICROSCOPY

Transmission electron microscopy is a microscopy technique in which a beam of electrons is transmitted through a specimen to form image. TEM images of Pure HAp and doped Mg samples were taken at. Sophisticated Analytical Instrument Facility (SAIF), Cochin. TEM

figures show the shape of the Synthesised samples .Fig. 4a-4c shows TEM micrographs of Pure HAp and Mg doped HAp

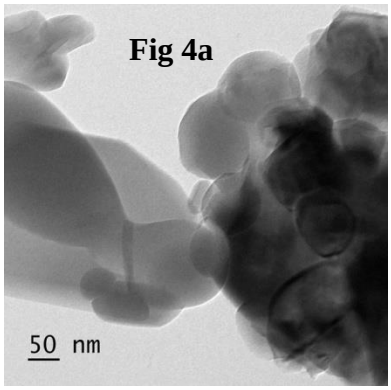

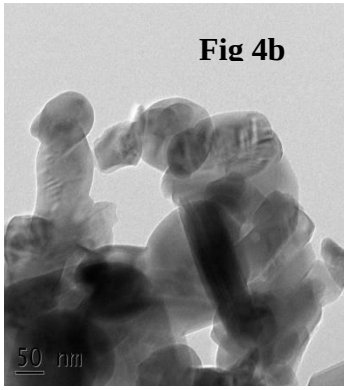

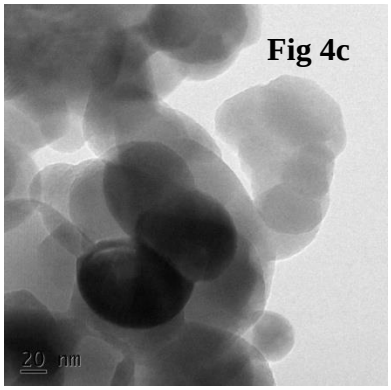

Fig4a – 4c. TEM images of $Ca_{10-x}Mg_x(PO_4)_6(OH)_2$ [x=0.0, 0.05, 0.10] nanostructures respectively.

3.5 Antimicrobial activity

Antibacterial activity of compounds against microbial pathogens using well diffusion method

Using Well diffusion method antimicrobial susceptibility testing was done at Venture Institute of Biotechnology and Bioinformatics Research Centre at Madurai**.** It was performed by sterilizing Mueller Hinton agar media. Antibacterial activity of the extract of compounds was determined using well diffusion method. It was performed by sterilizing Mueller Hinton agar media. After solidification, wells were cut on the Mueller Hinton agar using cork borer. The test bacterial pathogens were swabbed onto the surface of Mueller Hinton agar plates. Wells were impregnated with 25 µl of the test samples. The plates were incubated for 30 min to allow the extract to diffuse into the medium. The plates were incubated at 30^{o}C for 24 hours, and then the diameters of the zone of inhibition were measured in millimeters. The defence mechanisms of the body must be supported by the introduction of antibacterial factors, particularly antibiotic therapy. This type of therapy is performed using the oral route and is less effective: the dose of the antibiotic must be high in order to ensure its appropriate concentration around the inserted implant. Each antibacterial assay was performed in triplicate and mean values were tabulated. The results of antibacterial activity of shigella flexneri loaded hydroxyapatite. The zone of

inhibition around pure HAp against Shigella flexneri is given in Fig 5a-5c and inhibition is found around 0.05% .The zone of inhibition is clear at 0.10% . The zone of inhibition increases with increase in Mg doped HAp with loaded test organism. The 0.10% Mg doped HAp nanoparticles have the greater antibacterial activity than pure HAp. Reading of results was carried by measuring width of the zone of inhibition. The zone of inhibition increases with increase in Mg concentration. This result shows that doping of Mg enhances the antibacterial property of HAp. This factor is appreciable when HAp is implanted in the body for various medical purposes. The growth of inhibition against the clinical pathogen shigella flexneri for pure HAp and Mg doped HAp are shown in table 5.

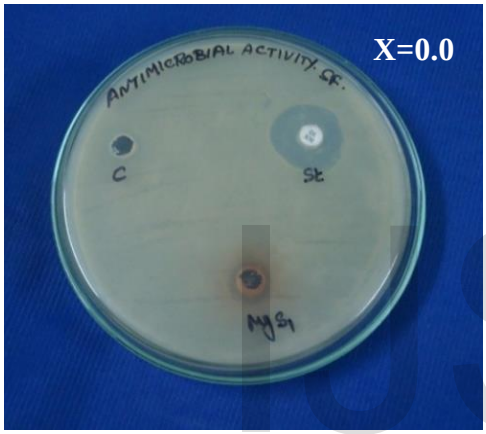

Fig4a Pure HAp

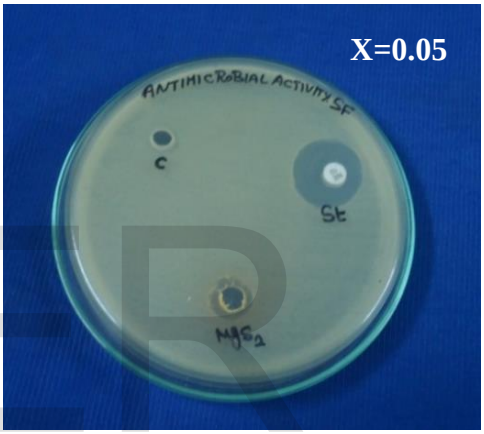

Fig4b 0.05% Mg doped HAp

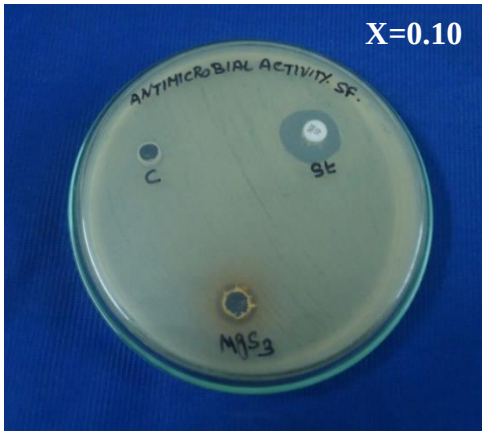

Fig4c 0.10% Mg doped HAp

Fig 5a -5c Zone of inhibition of $Ca_{10-x}Mg_x(PO_4)_6(OH)_2$ [x=0.0, 0.05, 0.10] nanostructures respectively.

Table 5 Zone of inhibition of $Ca_{10-x}Mg_x(PO_4)_6(OH)_2$ [x=0.0, 0.05, 0.10] nanostructures for the micro organism Shigella flexneri

Test organisms	Zone of inhibition in millimeter (in diameter)		
	X=0.0	X= 0.05	X=0.10
Shigella flexneri	12	14	15

Conclusion

Pure HAp and Mg doped samples were successfully synthesized by the solgel method. The results obtained in the XRD studies demonstrated that the Pure HAp and doped HAp powders synthesized by an adapted sol gel method gave hydroxyapatite with a good crystalline structure without any new phases or impurities. From XRD, using Debye Scherer's formula the average crystallite size was determined as 19nm to 21nm respectively. The crystallite size decreases from the pure HAp which may be due to the smaller atomic radius of Mg compared with calcium. The crystallite size was found by taking average for FWHM of all peaks of the samples. Doping of Mg causes structural changes which affect the crystalline nature of the sample. EDS figure and tables provide the elemental identification and quantitative compositional information. In FTIR spectrum the peaks show the presence of different elements. The presence of vibration and absorption bands are observed from FTIR .Microbial activity shows that the doping of Mg in HAp improves their antibacterial activity which is the desired property for medical applications.

REFERENCES

1. Characterization of Magnesium-Doped Hydroxyapatite Prepared by Sol-GelProcess", Salima Ziani, Samira Meski, and Hafit Khireddine,International Journal of Applied Ceramic Technology,.83-91

2. Khelendra Agrawal, Gurbhinder Singh, Devendra Puri, Satya Prakash Synthesis and Characterization of Hydroxyapatite Powder by Sol-Gel Method for Biomedical Application", 727-734.

3. Synthesis and thermal behavior of Mg-doped calcium phosphate nanopowders via the solgel method", A. Gozalian, A. Behnamghader, M. Daliri, A. Moshkforoush, Scientia Iranica F, (2011)1614–1622,

4. FTIR studies of chitosan acetate based polymer electrolytes Z.Osman, A.K. Arof Electrochimica Act 48 (2003) 993-999.

5. A.P. Brown, S. J. Milne,Sol-gel synthesis and characterisation of nano-scale Hydroxyapatite", Journal of Physics: M.Bilton1, (2012) 241, 012052.

6. Hydroxyapatite gels and nanocrystals prepared through a sol–gel process", Journal of Solid State Chemistry, A. Bigi, E. Boanini, and K. Rubini, (2004) 3092–3098,.

7. Antibacterial activities of HAp-TiO2 composites by Sol-Gel dipcoating technique. Mariappan, P. Pandi a, C. Gopinathanc, R. Rajeshwara Palanichamy, K.Neyvasagam Indian J. Res. Found., (2015) 4, 27-35. 2454-6577.

8. Synthesis and characterization of hydroxyapatite powder by sol–gel method for biomedical application, K. Agrawal, G. Singh, D. Puri, S. Prakash, and J. Miner. Mater.Charact. Eng. 10 (2011) 727–734.

9. S. Koutsopoulos, Synthesis and characterization of hydroxyapatite crystals: a review study on the analytical methods, J. Biomed. Mater. Res. 62 (2002) 600–612.

10. S.J. Kalita, H.A. Bhatt, Nanocrystalline hydroxyapatite doped with magnesium and zinc: synthesis and characterization, Mater. Sci. Eng. C 27 (2007) 837–848.

12. S. Nayar, M. K. Sinha, D. Basu, and A. Sinha, J. Mater. Sci.: Mater.Med. 17, 1063 (2006).

13. Q. Zhao, T. Wang, J. Wang, L. Zheng, T. Jiang, G. Cheng, and S. Wang, Appl. Surf. Sci. 257, 10126 (2011).

14. M. Percival, "Bone health & osteoporosis," Appl nutr sci rep, 5 [4] 1–6 (1999).

15. P.N. Kumta, C. Sfeir, D.-H. Lee, D. Olton, and D. Choi, “Nanostructured calcium phosphates for biomedical applications: novel synthesis and characterization.” [1] 65– 83 (2005).

16. Nagyné-Kovács, T.; Studnicka, L.; Kincses, A.; Spengler, G.; Molnár, M.; Tolner, M.; Lukács, I.E.; Szilágyi, I.M.;Pokol, G. Synthesis and characterization of Sr and Mg-doped hydroxyapatite by a simple precipitationmethod. Ceram. Int. (2018), 44, 22976-22982.

17. Drouet, C.; Carayon, M.-T.; Combes, C.; Rey, C. Surface enrichment of biomimetic apatites with biologically-active ions Mg2+ and Sr2+ a preamble to the activation of bone repair materials. Mater. Sci. Eng. C (2008), 28, 1544–1550.

18. Kannan, S.; Goetz-Neunhoe_er, F.; Neubauer, J.; Pina, S.; Torres, P.M.C.; Ferreira, J.M.F. Synthesis and structural characterization of strontium- and magnesium-co-substituted beta-tricalcium phosphate. (2010), 6, 571–576

19. Laurencin, D.; Almora-Barrios, N.; de Leeuw, N.H.; Gervais, C.; Bonhomme, C.; Mauri, F.; Chrzanowski, W.;Knowles, J.C.; Newport, R.J.;Wong, A.; et al. Magnesium incorporation into hydroxyapatite. Biomaterials (2011), 32, 1826–1837.

20. Fadeev, I.V.; Shvorneva, L.I.; Barinov, S.M.; Orlovskii, V.P. Synthesis and structure of magnesium-substituted hydroxyapatite. Inorg. Mater. (2003), 39, 947–950.

21. Landi, E.; Tampieri, A.; Mattioli-Belmonte, M.; Celotti, G. Biomimetic Mg-and Mg, CO3-substituted hydroxyapatites: Synthesis characterization and in vitro behavior. J. Eur. Ceram. Soc. (2006), 26, 2593–2601.

22. Adzila, S.; Ramesh, S.; Sopyan, I. Properties of magnesium doped nanocrystalline hydroxyapatite synthesize by mechanochemical method. ARPN J. Eng. Appl. Sci. (2016)11, 14097–14100.

23. Su, Y.; Li, D.; Su, Y.; Lu, C.; Niu, L.; Lian, J.; Li, G. Improvement of the biodegradation property and biomineralization ability of magnesium–hydroxyapatite composites with dicalcium phosphate dehydrate and hydroxyapatite coatings. ACS Biomater. Sci. Eng. (2016), 2, 818–828.

24. Adzila, S.; Murad, M.C.; Sopyan, I. Doping metal into calcium phosphate phase for better performance of bone implant materials. Recent Pat. Mater. Sci. (2012) 5, 18–47.

25. Percival, M. Bone health & osteoporosis. Appl. Nutr. Sci. Rep. (1999) 5, 1–6.

26. Tampieri, A.; Celotti, G.; Landi, E.; Sandri, M. Magnesium doped hydroxyapatite: Synthesis and characterization. Key Eng. Mater. (2004), 264, 2051–2054.